

Signal Processing With Temporal Sequences in Olfactory Systems

Andrzej G. Lozowski, *Member, IEEE*, Mykola Lysetskiy, *Student Member, IEEE*, and Jacek M. Zurada, *Fellow, IEEE*

Abstract—The olfactory system is a very efficient biological setup capable of odor information processing with neural signals. The nature of neural signals restricts the information representation to multidimensional temporal sequences of spikes. The information is contained in the interspike intervals within each individual neural signal and interspike intervals between multiple signals. A mechanism of interactions between random excitations evoked by odorants in the olfactory receptors of the epithelium and deterministic operation of the olfactory bulb is proposed in this paper. Inverse Frobenius–Perron models of the bulb’s temporal sequences are fitted to the interspike distributions of temporally modulated receptor signals. Ultimately, such pattern matching results in ability to recognize odors and offer a hypothetical model for signal processing occurring in the primary stage of the olfactory system.

Index Terms—Frobenius filter, interspike intervals, inverse Frobenius problem, Markov process, odorant concentration, olfactory bulb, shift map, temporal sequence.

I. INTRODUCTION

LIVING organisms perceive odors as sensations caused by mixtures of odorant molecules. Such molecules excite the olfactory receptors to respond with increased activity which is then passed on to the olfactory bulb for detection. Various odorant molecules excite different groups of receptors. A superposition of these excitations constitute the odor as detected by the olfactory bulb [1]. The relative concentrations of individual components constitute the odor type, whereas the absolute concentrations determine the odor intensity. The olfactory bulb has the task of transforming the input obtained from the receptors into a set of signals to be interpreted by the brain. The capacity of a simple discriminator to distinguish the target from background odorants has been statistically analyzed in [2].

The continuous quantities, such as molecule concentrations, cannot be directly represented by the signals produced by biological neurons. Neurons produce spikes and only indirectly their presence or absence, or time location may carry continuum of information. The nature of *neural signals* is assumed to have the following characteristics.

- 1) There is no significance of the shape of individual spikes. They simply mark instances of time when the neurons fire.

Manuscript received June 20, 2003; revised January 8, 2004. This work was supported by the U.S. Department of Navy Office of Naval Research under Grant N00014-01-1-0630.

A. G. Lozowski is with the Department of Electrical and Computer Engineering, Southern Illinois University, Edwardsville, IL 62026 USA.

M. Lysetskiy and J. M. Zurada are with the Department of Electrical and Computer Engineering, University of Louisville, Louisville, KY 40208 USA.

Digital Object Identifier 10.1109/TNN.2004.832730

- 2) The signal is a time sequence of spikes. Spikes may occur more or less frequently which has an effect on the average value of the signal.
- 3) Spikes may occur in a certain temporal pattern. More precisely, the inter-spike intervals may follow a distinct and repetitive behavior. This allows for code division of information conveyed by a single signal.
- 4) Two or more signals may exhibit cross correlation which typically results from synchronization between the signal sources. If the synchronized signals assume a certain spatial distribution, a set of such signals will manifest a spatio-temporal pattern.

The neural signals of the olfactory bulb representing the information about odors and intensities are further interpreted by the brain. The olfactory bulb functions as the first signal processing stage. In all nonbiological designs the first stage is responsible for the sensitivity and noise performance of the entire detection system. The same should hold true in case of the olfactory bulb. A very detailed investigation of neuronal noise and spike propagation can be found in [3].

The goal of this article is to identify the simplest method of encoding odor information in temporal sequences. The input–output interactions between temporal sequences can lead to an odor detection and encoding mechanism in the olfactory bulb.

II. TEMPORAL MODULATION ¹

The very input of the olfactory system, the epithelium, produces an enormous number of signals. Receptors are hard-wired to detect specific odor components and are uniformly distributed in the epithelium. The odor information is therefore, spatially distributed across the epithelium and is assumed to have no temporal dependency. Every odor and concentration can be represented by its “black and white photo” in which the gray levels of pixels encode spiking activities of the receptors. In this paper, the odor information is assumed to be spatially distributed and static, although there is a strong evidence of various significant aspects of the inhale–exhale rhythm and the impulse response of the olfactory bulb [5].

No temporal coding of information is performed by the individual receptors. Simply, the more molecules are present at the docking sites of the receptors, the more frequent their spiking. Based on response measurements and fitting of concentration–response curves presented in [6] and [7], the spiking frequency f of the receptors has an asymptotic dependency on the odorant concentration c (molarity). When the odorant concentration is

¹Term temporal modulation is adopted from [4].

at the lowest detectable level $c = c_t$, the receptor fires at the very slow rate of spontaneous activity. When the concentration grows infinitely large, the frequency reaches saturation at the maximum firing rate of f_m . The curve $f(c)$ fits the following definition:

$$f = \frac{2}{\pi} f_m \arctan \beta (c - c_t). \quad (1)$$

The slope factor β is expressed in terms of the dynamic range Δc defined as the odor concentration at which the frequency reaches 80% maximum, $f(c_t + \Delta c) = 0.8 f_m$. Given the dynamic range, the slope factor can be determined as $\beta = \tan(0.8\pi/2)/\Delta c$.

Concentration c , used in [6] and [7], is a logarithmic quantity related to the odorant molarity $c = \log m$, with m in mol/l. The investigated odorants were anisole (ANI), camphor (CAM), isoamyle acetate (ISO), and limonene (LIM). The curve fitting resulted in the following parameters for each odorant [6]:

	ANI	CAM	ISO	LIM
f_m	11 Hz	15 Hz	11 Hz	8 Hz
c_t	-6.7	-8.6	-7.0	-7.7
Δc	1.1	1.1	0.5	0.3.

Remarkably, linear curves are obtained if instead of spiking frequency f , the interspike intervals $\tau = 1/f$ are graphed versus the reciprocal of molarity, referred to as *sparsity* s . Since different odorants may have largely different molarity threshold levels $c_t = \log m_t$, the reciprocal of the incremental molarity $s = 1/(m - m_t)$ rather than the absolute value can be used in the joint graph for various odorants. The parametric representation of relationship (1) in the new coordinates (s, τ) for the introduced odorants is shown in Fig. 1. The horizontal and vertical axes are the incremental sparsity s and the interspike interval τ expressed in terms of molarity m as follows:

$$s(m) = \frac{1}{m - m_t} \quad (2)$$

$$\tau(m) = \left(\frac{2}{\pi} f_m \arctan \beta \log \frac{m}{m_t} \right)^{-1}. \quad (3)$$

As can be seen in the figure, diluting the odorant in the air increases the interspike intervals at an approximately constant rate. This may be regarded as temporal modulation with the conversion gain $G = d\tau/ds$, which is the slope of the line. The left side of each curve corresponds to the receptor saturation region. By extrapolating the curves to the intersections with the vertical axis, a minimum interval τ_0 for each receptor type can be found of value roughly around 100 ms. This minimum interval may be regarded the refractory period of the receptor. With just two parameters τ_0 and G for each receptor type, the temporal modulation illustrated in Fig. 1 can be readily described using first-order approximation:

$$\tau = \tau_0 + Gs. \quad (4)$$

The approximation can be validated only within the dynamic range of the receptor, that is, outside the saturation $s > 1/(m_t 10^{\Delta c})$.

III. ODOR CHARACTERIZATION WITH INTERSPIKE DISTRIBUTIONS

An odor is a superposition of a number of basic odorants. The concentration information is temporally modulated at the glomerular inputs of the olfactory bulb, therefore, the perception of odor intensity must be related to the interspike intervals. Increasing the odor intensity shortens the intervals at different rates for each basic odorant due to the differences in their conversion gains. This provides some explanation why responses of the mitral outputs can be different for the same odor at different intensities [8].

In the glomerular layer the enormous number of inputs converge into much less dimensional connections to the mitral cells. The glomeruli are also highly interconnected between each other via periglomerular interneurons [9]. Both inhibitory and excitatory connections are present within the glomeruli which indicates that a winner-take-all mechanism could be involved before the input to the mitral cells. The presence of such a mechanism would enable arranging of the input interspike intervals into distributions statistically representing the odor information.

Let R be the number of all types of receptors in the epithelium. This makes R also the number of distinct basic odorants, the basis for the odor space. Suppose the first four, out of all R odorants, are the ones shown in Fig. 1. An odor at a given intensity can be uniquely represented by a vector \mathbf{s} of sparsities of the basic odorants. For instance, an odor created by mixing 0.5 mol of CAM and 0.75 mol of LIM with 100 Ml of air would be represented by vector $\mathbf{s} = (\infty, 50, \infty, 75, \infty, \dots, \infty)$ Ml/mol. Vector $2\mathbf{s}$ would represent the same mixture diluted in twice the amount of air. In general, an odor, as seen by the epithelium, is $\mathbf{s} = (s_1, s_2, \dots, s_R)$. Terms “vector” and “basis” are understood to be suitable ways to arrange numbers rather than the strictly defined terms used in linear spaces.

A much more compressed way to describe odors is through distributions of interspike interval probabilities. This formalism may also be more relevant to the signals presented to the mitral inputs. Let the interspike intervals be quantized into N ranges with cutoff τ_{\max} . Interval τ_{\max} is considered to be a borderline between evoked and spontaneous activity of the receptors. A single neural signal can represent an odor with the interspike interval τ probability distribution $\mathbf{p} = (p_1, p_2, \dots, p_N)$, which is formally a vector of probabilities

$$p_n = \begin{cases} \Pr \left(\frac{n-1}{N} \tau_{\max} < \tau \leq \frac{n}{N} \tau_{\max} \right), & \text{if } n < N \\ \Pr(\tau_{\max} < \tau), & \text{if } n = N. \end{cases} \quad (5)$$

The quantized representation of the interspike interval distribution is chosen because it is more suitable for numeric computations than the probability density function. A satisfactory approximation of continuum can be achieved provided that N is large enough.

Suppose the 0.5 mol of CAM and 0.75 mol of LIM mixture with 100 Ml of air, indicated by the filled squares in Fig. 1, is presented to the olfactory epithelium. Two kinds of receptors would be activated, each responding with spikes separated by

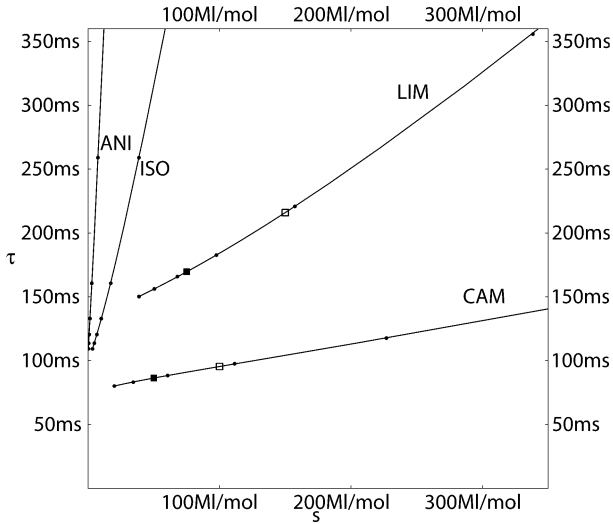


Fig. 1. Interspike intervals τ of receptor firing versus incremental sparsity s of odorant. Six points on each curve correspond to the following logarithmic concentration levels (left-to-right): $1.2\Delta c$, Δc , $0.8\Delta c$, $0.6\Delta c$, $0.4\Delta c$, and $0.2\Delta c$ above c_t . The axes units are ms and Ml/mol.

roughly 90-ms intervals and 175-ms intervals, respectively, according to Fig. 1. Suppose also that there is twice as many LIM receptors as those detecting CAM. In the winner-take-all competitions, the LIM receptors would have a better chance passing its signal compared to the CAM receptors. The described odor is represented by the filled bars of interspike interval probabilities in Fig. 2. The probability of the 175 ms LIM intervals is twice the probability of the 90 ms CAM intervals.

Suppose further that the same odor mixture is now diluted in twice the amount of air. This doubles the sparsity of the odor, hence, increasing the interspike intervals of both odorants present in the mixture. The diluted odors are represented in Fig. 2 by the empty bars of probabilities. Now the LIM intervals are about 220 ms and the CAM intervals increased to about 100 ms without a change to the probability levels. Note that the two odorants have different conversion gains and modulate the temporal intervals at different rates. As the odor intensity changes, this changes the probability pattern. A different hypothesis of time advance modulation where the resulting pattern is invariant under the concentration level was introduced in [10] and leads to functional models [11]. However, the neurophysiological evidence suggests that the patterns of bulbar activity actually do change when varying the odor intensity [8].

The signal processing occurring between the mitral cells and glomerular layer is a dynamical process. The information is embedded in the time realizations of signals. It may be retrieved only through observation of these signals for a period of time. The probability distribution of the interspike intervals may be retrieved by statistically analyzing the neural signals. Likewise, a simple stochastic process can be modeled to have the statistical properties representing a given odor through the probability distribution.

Suppose, in steady-state after all the transient response has vanished the odor is represented by the probability distribution \mathbf{p}^* defined according to (5). A Markov process [12] with the

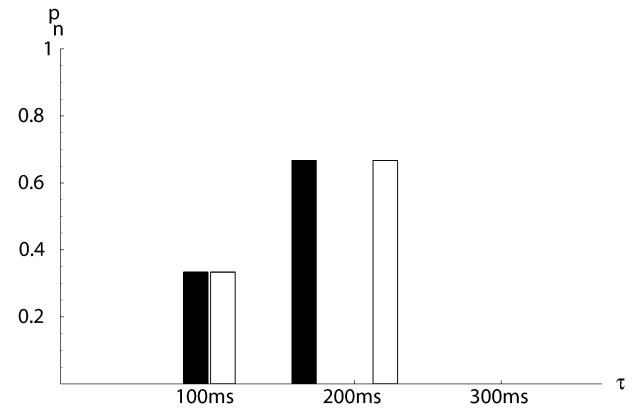


Fig. 2. Odor composed of 0.5 mol of CAM odorant and 0.75 mol of LIM odorant mixed with 100 Ml of air (filled bars) and then diluted in additional 100 Ml of air (empty bars). The bars have width τ_{\max}/N and represent probabilities of respective time intervals as defined by (5). Example with $N = 20$ and $\tau_{\max} = 350$ ms shown.

invariant distribution equal \mathbf{p}^* could serve as a first-order approximation of a dynamical system for that odor. Let $N \times N$ matrix P be the transition matrix of the Markov process

$$\mathbf{p}(k+1) = P\mathbf{p}(k). \quad (6)$$

Also, let the process converge to \mathbf{p}^* in a sense that $\mathbf{p}^* = \lim_{k \rightarrow \infty} \mathbf{p}(k)$ for almost every initial distribution $\mathbf{p}(0)$. The invariant distribution is the eigenvector of transition matrix P associated with the unit eigenvalue: $\mathbf{p}^* = P\mathbf{p}^*$. In this respect, the Markov process is a dynamical system in probabilistic space $S = \{\mathbf{p} \in [0; 1]^N \mid \sum_n p_n = 1\}$ with a stable fixed point \mathbf{p}^* . Further on, space S will be referred to as the odor space.

Consequently, an odor may be associated with an operator $P : S \rightarrow S$ in the odor space. The odor itself is the stable fixed point of the operator. There is a benefit of such a representation of odors. Operator P defines an odor indirectly through a definition of a dynamical system. It is easy and natural to generate realizations of neural signals using such operators, which is suitable in the modeling effort. There are many operators that have the same invariant distribution. Hence, the same odor information may be redundantly embedded in many different processes. Another approach to representing odors with Markov processes is presented in [13].

Formally, a realization of the introduced Markov process is a sequence of interspike intervals $\{\tau_k\}$. Define the interval range to be $T_n = [(n-1/N)\tau_{\max}; \tau_{\max}]$ if $n < N$, and $T_N = [\tau_{\max}; \infty)$ otherwise, where the interval range index n is defined in the same manner as in (5). For the sake of modeling through, optimization, a particular operator P may be developed to have \mathbf{p}^* as its invariant distribution of interspike intervals over time. Denote the elements of the operator by P_{ij} , so that $P = [P_{ij}]$, where i and j are the row and column indexes. Number P_{ij} is the probability that in the Markov process (6) an interval from the range T_i will follow the interval from the range T_j :

$$P_{ij} = \frac{\Pr(\tau_{k+1} \in T_i \text{ and } \tau_k \in T_j)}{\Pr(\tau_k \in T_j)}. \quad (7)$$

There is no closed-form formula for selecting P_{ij} s for a given \mathbf{p}^* . However, starting with some random P_{ij} s, an optimization algorithm can be used to find the P_{ij} s as the minimum of a suitable cost function. Since all P_{ij} s are probabilities, they must be numbers in the unit segment from 0 to 1. This fact allows for constructing one of the components to be included in the cost function, namely, the unit segment potential. For each number P_{ij} , a potential function $v(P_{ij})$, shown in Fig. 3, describes how distant P_{ij} is from the unit segment

$$v(P_{ij}) = \frac{(2P_{ij} - 1)^2}{1 + (2P_{ij} - 1)^{-6}}. \quad (8)$$

Function v attains the minimum in the middle of the unit segment and is maximally flat within the segment. The maximally flat approximation [14] with a rational function is chosen to facilitate the optimization process. The partial costs $v(P_{ij})$ sum up to the cost function component $E_v(P)$ responsible for keeping all the entries of P within the unit segment

$$E_v(P) = \sum_{i=1}^N \sum_{j=1}^N v(P_{ij}). \quad (9)$$

Operator P is a probabilistic matrix in a sense that all its column vectors are normalized probability distributions. Therefore, the column sums of P must sum up to 1. Another cost function component $E_c(P)$ measures the deviation from this requirement

$$E_c(P) = \sum_{j=1}^N \left(1 - \sum_{i=1}^N P_{ij} \right)^2. \quad (10)$$

If operator P is a well defined transition matrix of Markov process (6), then the cost sum $E_v(P) + E_c(P)$ is low and close to its minimum attainable value. The goal of the cost minimization procedure is to develop operator P with the constraint that \mathbf{p}^* is its principal eigenvector associated with eigenvalue 1. To simplify the operator synthesis, matrix P will be assumed to be diagonalizable: $P = B\Lambda B^{-1}$. The diagonal matrix $\Lambda = \text{diag}(\boldsymbol{\lambda})$ is composed of N eigenvalues $\boldsymbol{\lambda} = (\lambda_1, \lambda_2, \dots, \lambda_N)$ of P . Let $\lambda_1 = 1$. The convergence rate of the dynamical system (6) heavily depends on the radius of the remaining λ_i s for $i > 1$. Operator P is synthesized with random λ_i s, for $i > 1$, with the assumption that $|\lambda_i| < r < 1$ and the radius r is kept low to improve the convergence rate. In the numerical experiment r was selected to be equal to 0.2. Operator P is diagonal in the basis constructed with the column vectors of B . Since $\lambda_1 = 1$, the first column vector of B is \mathbf{p}^* . More precisely, $B_{ij} = p_i^*$ for $j = 1$. All other entries B_{ij} , for $j > 1$, are variables in the optimization process. Their initial values are selected randomly from the uniform distribution in the range $(-1; 1)$. Final matrix B is found using an optimization algorithm to minimize the cost function as in the following expression:

$$\min_{B_{ij}|j>1} [E_v(P) + E_c(P)]. \quad (11)$$

The minimized solution oftentimes needs a final touch to make sure that P has no negative entries, no entries greater than one and that column sums of P are indeed 1. This can be done by

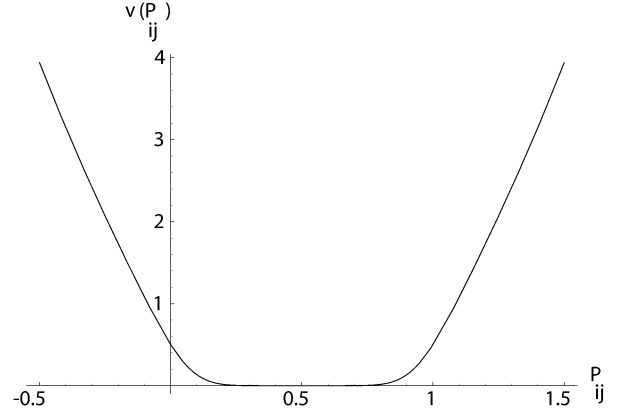


Fig. 3. Unit segment potential function. In the total cost function, numbers $P_{ij} \in [0; 1]$ contribute much less than numbers P_{ij} outside this range. Minimization of w will attract all P_{ij} s toward the inside of the unit segment.

zeroing of negative values and normalization of columns. The principal eigenvector of P is not very sensitive to such trimming of P .

IV. EMBEDDING DISTRIBUTIONS IN TEMPORAL SEQUENCES

As illustrated in the example shown in Fig. 2, the probabilistic representation of odors and intensities fits well the random nature of excitations received from the olfactory epithelium. The Markov model is also a natural candidate for a simple approximation of the dynamics behind spike interactions driven by the receptors. The olfactory bulb, however, should be considered a deterministic system which has no random variables other than the input received from the epithelium. Moreover, the olfactory bulb is capable of self-excitatory activity in response to the input. This may be the factor contributing to both high sensitivity and high selectivity of the sense of smell [15]. From this perspective, it seems reasonable to regard the olfactory bulb as an active medium rather than a passive relay of receptor signals. The olfactory bulb actively produces firing activity in response to the receptor signals [16].

A sequence of interspike intervals complying with a given interval distribution can be generated in a deterministic dynamical system. The simplest such system is a one-dimensional map constructed by solving the inverse Frobenius–Perron problem [17]. The overall goal of the search for a sequence generator is to be able to represent the odor information by a distribution of interspike intervals. A simple shift map can be constructed directly from the probabilistic operator used in approximation (6), as described in detail in [18].

First, a piecewise linear map $f : [0; N] \rightarrow [0; N]$, $[0; N] \subset \mathbb{R}$ is derived from probabilities included in the operator P

$$f(x) = \frac{1}{P_{ij}} \left(x - j + \sum_{m=1}^i P_{mj} \right) + N - i, \quad (12)$$

$$\text{if } j - \sum_{m=1}^i P_{mj} \leq x < j + P_{ij} - \sum_{m=1}^i P_{mj}.$$

As shown in Fig. 4, map f is composed of N^2 linear segments corresponding to N^2 numbers P_{ij} . The slopes of the segments are simply $1/P_{ij}$. To evaluate $f(x)$, the pair of indexes i and j

appropriate for a given x needs to be identified using the condition provided by (12).

By scaling the domain and range of map f , the dynamical system generating temporal sequence $\{\tau_k\}$ can be defined with the help of shift map h

$$h(\tau) = \frac{\tau_{\max}}{N-1} f\left(\frac{N-1}{\tau_{\max}}\tau\right). \quad (13)$$

Regardless of the initial condition chosen, subsequent mappings with h will determine sequence $\{\tau_k\}$ whose distribution of values converges to the invariant distribution of process (6). A deterministic dynamical system

$$\tau_{k+1} = h(\tau_k) \quad (14)$$

may be regarded as a generator of realizations of neural signals for a given distribution of interspike intervals.

A numeric example of shift-map synthesis is shown in Fig. 5. Three interspike-interval distributions \mathbf{p}_A^* , \mathbf{p}_B^* , and \mathbf{p}_C^* are selected randomly to characterize three hypothetical odors A, B, and C. The bars represent probabilities p_n of respective time intervals as defined by (5). The horizontal axis is normalized such that interval $N\tau_{\max}/(N-1)$ corresponds to 1. Shift maps h_A , h_B , and h_C are evaluated for the example odors and shown in the middle row of figures also in time-normalized coordinates. The maps have N disconnected branches, however, vertical lines connecting the branches are added to enhance the graphs. Starting with a random initial interval, each map iterated 3000 times according to (14) produced a temporal sequence. The sequences are shown in the bottom row of figures. Each interval in a sequence is indicated as a point whose vertical coordinate is the normalized time. This way the density of points reflects the original distribution plots if rotated clockwise by 90° .

V. FROBENIUS FILTER FOR TEMPORAL SEQUENCES

It is broadly accepted that the olfactory bulb provides support for a pattern recognition mechanism for odor detection and classification. Not all of the recognition is taking place there, but definitely the process is initiated in the olfactory bulb. Assuming that the temporal sequences of interspike intervals are carriers of odor information, an implementation of signal processing system (14) can be proposed. Ultimately, the goal is to demonstrate usefulness of the proposed mechanism in odor recognition.

The signal processing scheme shown in Fig. 6 will be referred to as the Frobenius filter. The input to the filter is a temporal sequence whose interspike intervals are determined by the random variable τ_{in} with values governed by the probability distribution \mathbf{p}_{in} defined as in (5). Distribution \mathbf{p}_{in} characterizes an odor.

The Frobenius filter is simply a shift map with the feedback loop controlled by a random switch. The switch operation is described by a two-valued stochastic process $\xi : \{0, 1\} \times N \rightarrow R$. The filter is producing time intervals based on the switch position. At every interval k , the switch position depends on the value of ξ_k governed by probabilities

$$\Pr(\xi_k = 1) = c \quad (15)$$

$$\Pr(\xi_k = 0) = 1 - c \quad (16)$$

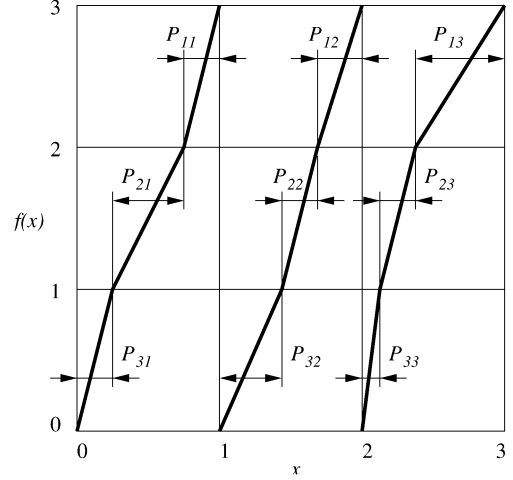


Fig. 4. Example of a piecewise linear shift map $f(x)$. Function f is composed of N continuous branches $f_j : [j-1; j] \rightarrow [0; N]$. If x is chosen randomly from the uniform distribution over the range $(0; N)$, the conditional probability P_{ij} that $f(x) \in (i-1; i)$ given the fact $x \in (j-1; j)$ can be evaluated by $P_{ij} = \|f_j^{-1}([i-1; i])\|$. Example with $N = 3$ shown.

where $c \in [0; 1]$ is a constant parameter. When $\xi_k = 1$, the filter is receiving the input τ_{in} . The opposite position of the switch ($\xi_k = 0$) lets the shift map determine the output time interval based on the previous interval as in (14). The overall filter equation reads

$$\tau_{k+1} = h[\xi_k \tau_{\text{in}} + (1 - \xi_k) \tau_k]. \quad (17)$$

The notion of the switch is an attempt to model a competition between the input and the feedback. Its random operation is inherited from the random nature of the input temporal sequence.

The three shift maps h_A , h_B , and h_C , introduced in Fig. 5, are used to illustrate the function of the Frobenius filter. Each of the shift maps was stimulated at the input by values generated by probability distributions \mathbf{p}_A^* , \mathbf{p}_B^* , and \mathbf{p}_C^* representing three different odors. Fig. 7 shows all possible input-filter combinations arranged in the following nine pairs:

$$\begin{array}{ccc} (\mathbf{p}_A^*, h_A) & (\mathbf{p}_B^*, h_A) & (\mathbf{p}_C^*, h_A) \\ (\mathbf{p}_A^*, h_B) & (\mathbf{p}_B^*, h_B) & (\mathbf{p}_C^*, h_B) \\ (\mathbf{p}_A^*, h_C) & (\mathbf{p}_B^*, h_C) & (\mathbf{p}_C^*, h_C). \end{array} \quad (18)$$

In each instance, $K = 20000$ values random values τ_{in} were drawn from the input distribution and applied with probability $c = 0.5$ to the filter. The values drawn were also sorted in the ascending order and stored. In the sorted input sequence $\{u_i\}$ the following property holds: $i < j \Rightarrow u_i \leq u_j$. When plotted, the graph of the sorted sequence would resemble the shape of the cumulative distribution function of the random variable τ_{in} .

The realization of the sequence $\{\tau_k\}$ generated by the Frobenius filter for K iterations were also sorted in the same manner. The sorted output sequence $\{t_i\}$ was then compared to the sorted input sequence in Fig. 7. More precisely, the graphs in the figure are the sequences of quadratic distances $\{(u_i - t_i)^2\}$ in each of the nine instances. The horizontal line is the mean-square value of the distance $(u_i - t_i)^2$. As seen in the figure, the input-output sequences generated in pairs

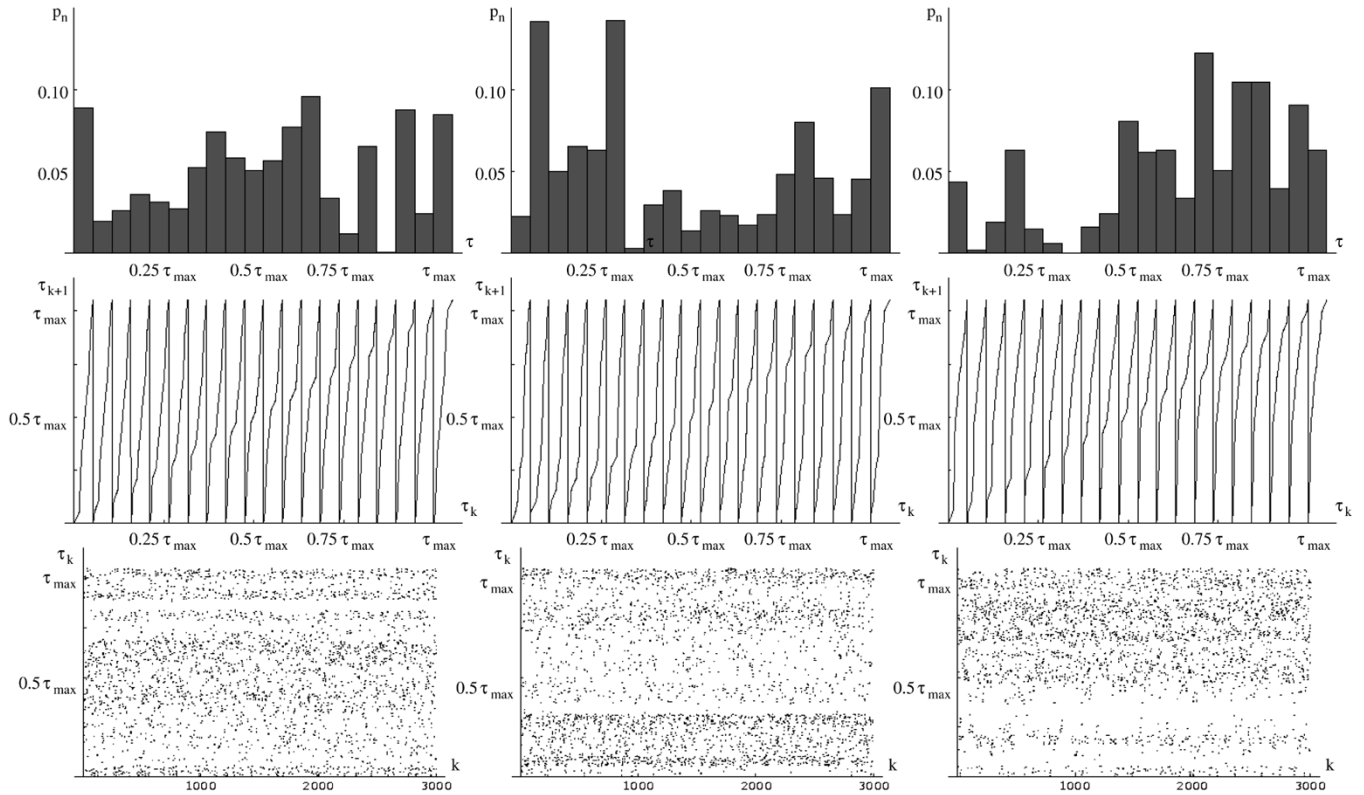


Fig. 5. Synthesis of temporal-sequence generators. Three example interspike-interval distributions with $N = 20$ representing three different odors are shown in the top row. The corresponding shift maps and distributions of values of generated temporal sequences are shown underneath. The time interval axes are normalized to the range of $(0; 1)$. Each graph in the bottom row contains 3000 points representing interspike intervals placed vertically according to the length of the interval.

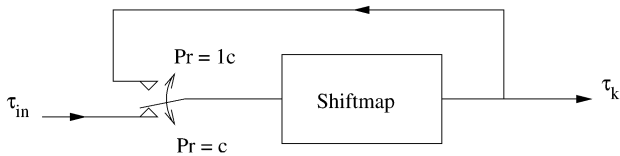


Fig. 6. Frobenius filter is a shift map with input. Either the input interval τ_{in} or the present output interval τ_k is transformed into the next output interval τ_{k+1} .

(\mathbf{p}_A^*, h_A) , (\mathbf{p}_B^*, h_B) , and (\mathbf{p}_C^*, h_C) are synchronized in a sense that the quadratic distance between input and output interval distributions is small. The distances in all the other pairs are significantly larger. By detecting low distance between the input and the output of the filter, an odor recognition mechanism can be devised.

Two examples of realizations of the input and output temporal sequences are shown in Figs. 8 and 9. The proposed mechanism uses a pattern matching phenomenon which signals successful detection as a decreased distance between parameters of the input and the output neural signals. The pattern matching is not based on coherence of the two signals. As shown in the figures, no similarity in realizations of the input and the output can be observed in either the matched or unmatched odor-filter pairs. In case of the matched pair, the similarity is in the statistical properties of the input and the output signals.

Value $c = 0.5$ used in the experiment is the midpoint of the probability range. The value of c may be selected to optimize the performance with respect to different numbers of odors and

filters. The extremes correspond to no-input ($c = 0$) and the open-loop ($c = 1$) conditions. In this regard, c represents the strength of the input coupling. With no input, the entire system becomes a simple pattern-matching mechanism. In the open-loop condition, the output is driven by the input through the filter mapping h . In both cases if the input is a stationary process, the filter output is also stationary and the distance $u_i - t_i$ can be evaluated. However, there will be no gain resulting from the synchronizing effect imposed by the switch.

VI. CONCLUSION

The details of how the cells of the olfactory bulb could encode the information in the way described in this paper are not discussed here. The goal set for this work was to describe the simplest method of encoding information in temporal sequences and show the input-output interactions which can lead to an odor detection and encoding mechanism. All the computations are very simple. No memory is necessary, only the last time interval is locally kept in the evaluation of the next time interval in the output sequence. Actual neurons are capable of performing such a storage with their inherent leaky integration.

The computational complexity of the model depends on the resolution N of the interspike interval distributions. It determines the dimensionality of the Markov transition matrix. Minimization (11) is the most time-demanding computation involved in the approach and takes a significant amount of time to evaluate. The minimization may be regarded as the learning process.

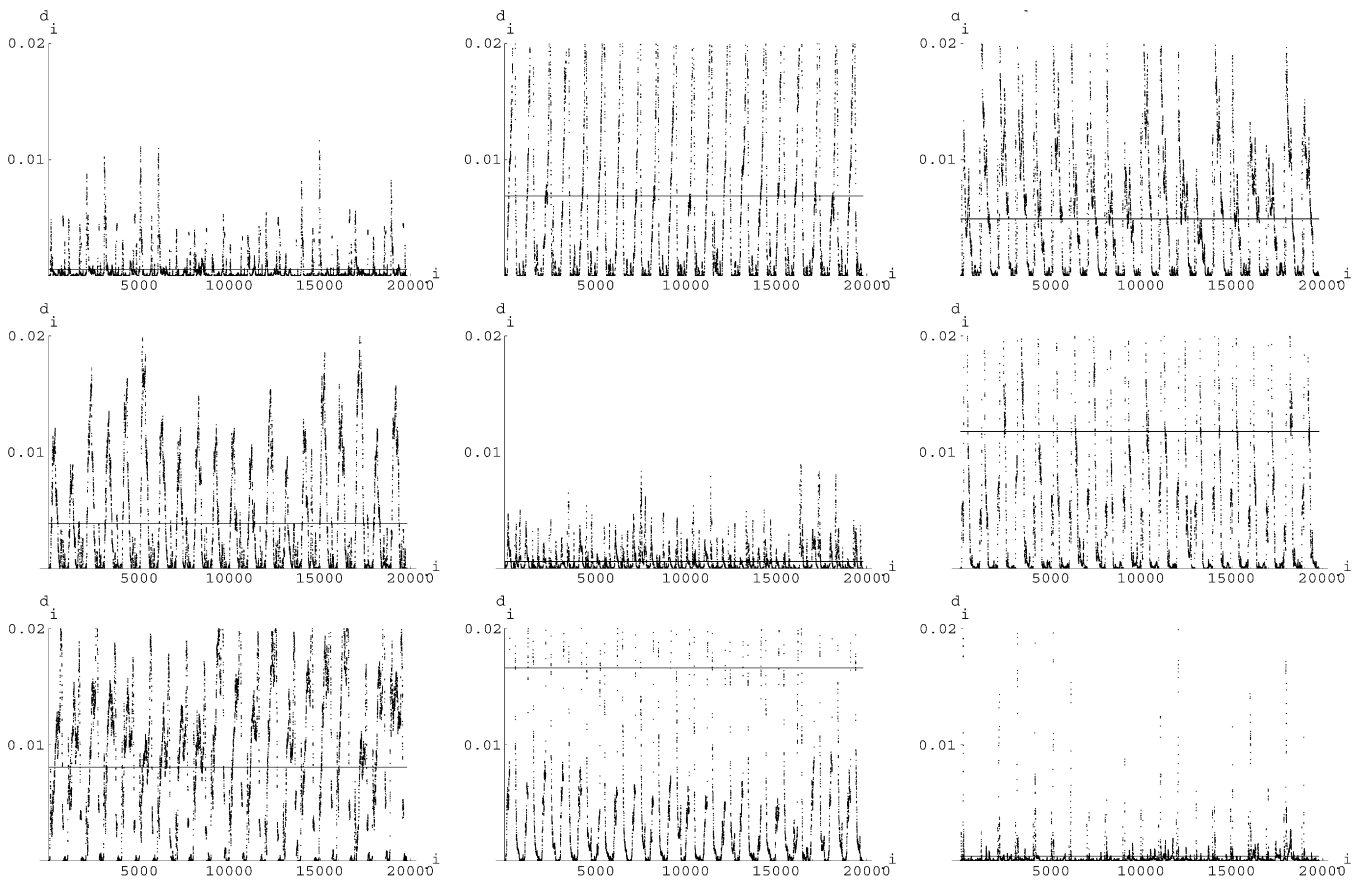


Fig. 7. Nine instances of a Frobenius filter stimulated by an input distribution for 20 000 iterations. Quadratic distance $d_i = (u_i - t_i)^2$ between cumulative distributions of interspike intervals at input u_i and output t_i of the filter shown. The graphs are arranged according to (18).

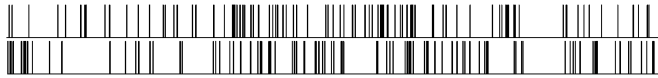


Fig. 8. Realizations of the input (top) and output (bottom) temporal sequences for a matched pair (p_A^*, h_A) . A fragment containing 100 spikes shown.

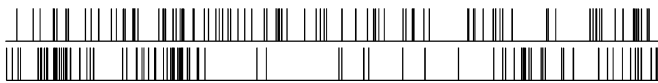


Fig. 9. Realizations of the input (top) and output (bottom) temporal sequences for unmatched pair (p_B^*, h_A) . A fragment containing 100 spikes shown.

The shapes of the shift maps shown in Fig. 5 are not crucial for in the operation of the Frobenius filters. The proposed shapes are just samples of infinite possibilities chosen for mathematical simplicity. In fact, any mapping that is mixing and expanding [19] can be used in the Frobenius filter. Such mappings develop continuous invariant distributions and guarantee ergodicity of the temporal sequence in a sense that the invariant distribution is reachable from any initial condition. Temporal sequences at the output of the filter have a very strong ability of encoding information in the time scale. It is sufficient to isolate just a few consecutive spikes to be able to identify the shift map which generated the spikes and effectively identify the encoded odor.

ACKNOWLEDGMENT

The authors would like to acknowledge inspiring discussion and help from Prof. J. S. Kauer, Tufts University School of Medicine, Medford, MA.

REFERENCES

- [1] T. A. Dickinson, J. White, J. S. Kauer, and D. R. Walt, "Current trends in 'artificial-nose' technology," *Trends Biotechnol.*, vol. 16, no. 6, pp. 250–258, June 1998.
- [2] N. Caticha, J. E. P. Tejada, D. Lancet, and E. Domany, "Computational capacity of an odorant discriminator: The linear separability of curves," *Neural Computat.*, vol. 14, pp. 2201–2220, 2002.
- [3] A. Manwani and C. Koch, "Detecting and estimating signals in noisy cable structures, I: Neuronal noise sources," *Neural Computat.*, vol. 11, pp. 1797–1829, 1999.
- [4] R. W. Friedrich and G. Laurent, "Dynamic optimization of odor representations by slow temporal patterning of mitral cell activity," *Science*, vol. 291, pp. 889–894, Feb. 2001.
- [5] J. S. Kauer, "Real-time imaging of evoked activity in local circuits of the salamander olfactory bulb," *Nature*, vol. 331, pp. 166–168, July 1988.
- [6] J. P. Rospars, P. Lansky, P. Duchamp-Viret, and A. Duchamp, "Spiking frequency versus odorant concentration in olfactory receptor neurons," *BioSystems*, vol. 58, pp. 133–141, 2000.
- [7] —, "Characterizing and modeling concentration-response curves of olfactory receptor cells," *Neurocomput.*, vol. 38–40, pp. 319–325, 2001.
- [8] J. White, K. A. Hamilton, S. R. Neff, and J. S. Kauer, "Emergent properties of odor information coding in a representational model of the salamander olfactory bulb," *J. Neurosci.*, vol. 12, no. 5, pp. 1772–1780, May 1992.
- [9] J. S. Kauer, "Contributions of topography and parallel processing to odor coding in the vertebrate olfactory pathway," *Trends Neurosci.*, vol. 14, no. 2, pp. 79–85, Feb. 1991.

- [10] J. Hopfield, "Pattern recognition computation using action potential timing stimulus representation," *Nature*, vol. 376, pp. 33–36, July 1995.
- [11] M. Lysetskiy, A. Lozowski, and J. M. Zurada, "Invariant recognition of spatio-temporal patterns in the olfactory system model," *Neural Process. Lett.*, vol. 15, pp. 225–234, June 2002.
- [12] A. G. Lozowski and B. L. Noble, "Processing temporal sequences," in *Proc. 45th Midwest Symp. Circuits and Systems (MSCAS'02)*, vol. 1, Tulsa, Oklahoma, Aug. 4–7, 2002, pp. 180–183.
- [13] B. Quenet and D. Horn, "The dynamic neural filter: A binary model of spatiotemporal coding," *Neural Computat.*, vol. 15, pp. 309–329, 2003.
- [14] A. Budak, *Passive and Active Network Analysis and Synthesis*. Prospect Heights, IL: Waveland Press, 1991.
- [15] T. A. Dickinson, J. White, J. S. Kauer, and D. R. Walt, "A chemical-detecting system based on a cross-reactive optical sensor array," *Nature*, vol. 382, pp. 697–700, Aug. 1996.
- [16] J. White, T. A. Dickinson, D. R. Walt, and J. S. Kauer, "An olfactory neuronal network for vapor recognition in an artificial nose," *Biol. Cybern.*, vol. 78, no. 4, pp. 245–251, Apr. 1998.
- [17] E. M. Bollt, "Controlling chaos and the inverse Frobenius-Perron problem: Global stabilization of arbitrary invariant measures," *Int. J. Bifurcation Chaos*, vol. 10, no. 5, pp. 1033–1050, 2000.
- [18] D. Pingel, P. Schmelcher, and F. K. Diakonov, "Theory and examples of the inverse Frobenius-Perron problem for complete chaotic maps," *Chaos*, vol. 9, no. 2, pp. 357–366, 2000.
- [19] G. Mazzini, R. Rovatti, and G. Setti, *Chaos-Based DS-CDMA: Introduction. Some Tools for Studying Chaos With Densities*. Berkeley, CA: Univ. of California Press, 2000.



Andrzej G. Lozowski (S'96–M'99) received the M.S. degree in electrical engineering with specialization in electronic circuits from the Warsaw University of Technology, Warsaw, Poland, in 1994, and the Ph.D. degree in computer science and engineering from the University of Louisville, Louisville, KY, in 1999.

He is currently an Assistant Professor and the Graduate Program Director in the Department of Electrical and Computer Engineering, Southern Illinois University, Edwardsville, IL. His research interests include nonlinear dynamics, analog circuit design and signal processing.

Mykola Lysetskiy (S'99) received the M.S. degree in physics from Kharkov State University, Kharkov, Ukraine, in 1997, and the Ph.D. degree in computer science and engineering from the University of Louisville, KY, in 2003.

He is presently a Postdoctoral Researcher in the Department of Anatomy and Neurobiology, University of California, Irvine.



Jacek M. Zurada (M'82–SM'83–F'96) is the S.T. Fife Alumni Professor of Electrical and Computer Engineering, University of Louisville, Louisville, KY. He is the coeditor of *Knowledge-Based Neurocomputing* (Cambridge, MA: MIT Press, 2000), *Computational Intelligence: Imitating Life* (Piscataway, NJ: IEEE Press, 1994), and the author of *Introduction to Artificial Neural Systems* (Boston, MA: PWS-Kent, 1992). He is the author or coauthor of more than 200 journal and conference papers in the area of neural networks and VLSI circuits.

Dr. Zurada has been the Editor-in-Chief of the IEEE TRANSACTIONS ON NEURAL NETWORKS since 1998. He was the recipient of the 2001 University of Louisville President's Distinguished Service Award for Service to the Profession. He is currently the President of the IEEE Neural Networks Society for 2004–2005. In March 2003, he was conferred the Title of the Professor by the President of Poland, A. Kwasniewski.